Environmental Science & Technology

Article

pubs.acs.org/est

Visible Light Sensitized Production of Hydroxyl Radicals Using Fullerol as an Electron-Transfer Mediator

Jonghun Lim,[†] Hyejin Kim,[†] Pedro J. J. Alvarez,[‡] Jaesang Lee,*[,§] and Wonyong Choi*[,†]

[†]Division of Environmental Science and Engineering, Pohang University of Science and Technology (POSTECH), Pohang 37673, Korea

[‡]Department of Civil & Environmental Engineering, Rice University, Houston, Texas 77005, United States

[§]School of Civil, Environmental, and Architectural Engineering, Korea University, Seoul 136-701, Korea

* Supporting Information

ABSTRACT: Fullerenes and their derivatives are known to photosensitize the production of singlet oxygen ($^1O_2$), but their role in generating hydroxyl radical ($^{\bullet}OH$) under visible light has not been reported. Here, we demonstrate that fullerol can mediate the electron transfer from Rhodamine B dye to O_2 under visible light irradiation, achieving simultaneous dye decolorization and $^{\bullet}OH$-induced degradation of 4-chlorophenol. The hydroxyl radical is proposed to be produced via a consecutive reduction of molecular oxygen by fullerol anion radical, which is formed through the electron transfer from the dye to the triplet state of fullerol. Mechanistic investigations using various probe reagents such as superoxide dismutase (superoxide quencher), t-butanol ($^{\bullet}OH$ quencher), and coumarin ($^{\bullet}OH$ probe) provided indirect evidence for the generation of $^{\bullet}OH$ under visible light. Furthermore, spin trapping technique directly detected the oxidizing species such as $^{\bullet}OH$, $HO_2^{\bullet}$, and $^1O_2$ in the visible light irradiated solution of RhB/fullerol mixture. It was proposed that the photochemical oxidation mechanism depends on pH: $^{\bullet}OH$ production is favored at acidic pH through fullerol-mediated sequential electron transfer while $^1O_2$ is generated as a main oxidant at neutral and alkaline condition through the energy-transfer process. Therefore, the photochemical oxidation can be switchable between $^{\bullet}OH$-driven and $^1O_2$-driven mechanism by a simple pH adjustment.

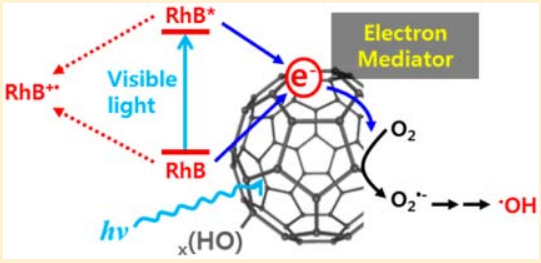

INTRODUCTION

The photosensitizing activity of C_{60} fullerenes to mediate energy and electron transfer enables the production of various reactive oxygen species (ROS) under visible light irradiation.[1−4] Superoxide radical anion ($O_2^{\bullet-}$) is generated when C_{60} in Triton X100 surfactant matrix is photochemically excited in the presence of trimethylamine as an electron donor.[5] Photon energy transfer from the triplet state of C_{60} derivatives to dissolved oxygen produces singlet oxygen ($^1O_2$) in aqueous media.[6−8] Whereas water-stable C_{60} aggregates exhibit insignificant photochemical properties via triplet−triplet annihilation and self-quenching mechanism,[5,9] ozone-treated products of C_{60} that are introduced with the oxygen-containing functionalities on the cage structure are reported to generate ROS to inactivate for Escherichia coli under black light irradiation.[10]

Despite the photosensitizing activity of pristine C_{60} for ROS generation, the hydrophobicity and the extremely low solubility of pristine C_{60} in water (log K_{ow} = 6.67)[11] limit its application for photochemical treatment of water. Thus, chemical derivatization has been attempted to make C_{60} soluble in water and to hinder its dense clustering, which significantly lowers the efficiency of C_{60} mediated energy transfer.[9] Multihydroxylated fullerene (i.e., fullerol) is well soluble in water and has been demonstrated to produce $^1O_2$ for photochemical inactivation of MS-2 bacteriophage.[12] A comparative study using various C_{60} derivatives demonstrated superior performance of aminofullerene in $^1O_2$-induced decomposition of selected pharmaceutical compounds and inactivation of MS-2 phage under visible light irradiation.[7] Furthermore, the recovery and recycling of fullerene-based sensitizers after photochemical treatment of organics in water are enabled by their immobilization on functionalized silica and mesoporous silica supports containing nanosized magnetite.[13,14]

Another interesting property of C_{60} derivatives is the electron-shuttling capability in photochemical redox systems, which has been rarely employed in the rational design of fullerene-based photochemical treatment processes for the following reasons. First, superoxide formed via one-electron transfer to dissolved oxygen provides a minor degradative pathway because of the mild oxidizing power [$E^0(O_2^{\bullet-}/H_2O_2)$ = 0.89 V_{NHE}].[15] Second, the C_{60} mediated electron transfer requires the presence of electron-donating substrates. However, organic pollutants as an electron donor may be utilized along

Received: June 30, 2016
Revised: August 31, 2016
Accepted: September 2, 2016
Published: September 2, 2016

DOI: 10.1021/acs.est.6b03250
Environ. Sci. Technol. 2016, 50, 10545−10553

with C_{60} derivatives in inducing the fullerene-mediated electron transfer for ROS production. Dye (representing a major class of recalcitrant pollutants) that readily undergoes visible light induced sensitization to donate electrons (i.e., oxidatively decolorized) is an ideal test substrate for this purpose. In such system, water-soluble C_{60} derivatives would facilitate the transfer of electrons from the visible light excited dyes to O_2, achieving concurrent dye decolorization and ROS (e.g., $^{\bullet}OH$) production (see Scheme 1). A possible role of C_{60} as an electron shuttle was proposed from a study of photosensitized production of hydroperoxyl radical ($HO_2^{\bullet}$) from H_2O_2 in the dye/C_{60} system in which water-stable C_{60} clusters enable the delivery of electrons from the UV-excited dyes to H_2O_2.[16] Other studies also found that C_{60} derivatives readily accept electrons from the excited dye sensitizers.[16,17] Such previous results raise a possibility of utilizing consecutive transfer of electrons to dioxygen via C_{60} as a method to generate $^{\bullet}OH$ radical in the dye/C_{60} system. The production of nonselective $^{\bullet}OH$ that enables the oxidative degradation of a broad range of organic contaminants is essentially needed in the development of efficient advanced oxidation processes (AOPs).

Scheme 1. Main Photosensitized Oxidation Pathways and the Relative Energy States for Fullerol[a]

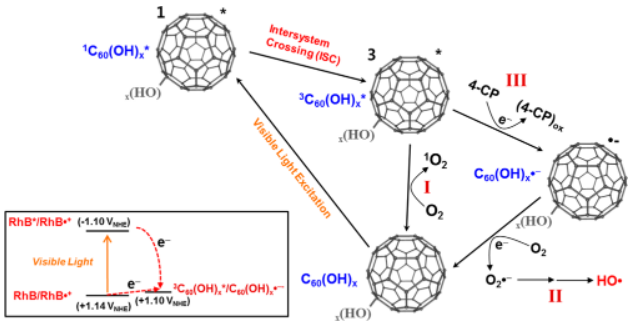

[a]I, singlet oxygen production; II, hydroxyl radical production; III, direct electron transfer.

In this study, we propose and attest the hypothesis that fullerol as an electron shuttle can mediate the successive reduction of dioxygen to $^{\bullet}OH$ via the sensitization of a dye, Rhodamine B (RhB), by monitoring the simultaneous decolorization of RhB and the decomposition of 4-chlorophenol (4-CP) under the visible light irradiation ($\lambda > 420$ nm). The effects of experimental parameters such as photoexcitation wavelengths, pH, and various probe reagents on the concurrent degradation of RhB and 4-CP were systematically investigated to understand the overall photochemical mechanisms.

MATERIALS AND METHODS

Chemicals and Materials. Fullerol ($C_{60}(OH)_x(ONa)_y$, with $x + y = 24$, $y = 6 - 8$) was purchased from MER corporation (Tucson, AZ). The chemicals used in this work were 4-chlorophenol (4-CP, Sigma), Rhodamine B (RhB, Aldrich), furfuryl alcohol (FFA, Aldrich), dichloroacetate (DCA, Aldrich), tetramethylammonium chloride (TMA, Acros), $Na_2Cr_2O_7$ (Cr(VI), Aldrich), tert-butanol (t-BuOH, Aldrich), hydrogen peroxide (H_2O_2, Junsei), superoxide dismutase from bovine erythrocytes (SOD, Sigma), L-histidine (Sigma), coumarin (Sigma), 5,5-dimethyl-1-pyrroline-N-oxide (DMPO, SCI), 2,2,6,6-tetramethyl-4-piperidone (TEMP, Aldrich), and deuterium oxide (D_2O, Aldrich). All chemicals were used as received without further purification. Ultrapure deionized water (18 MΩ-cm) was used to prepare all aqueous solutions. Argon gas purging of the aqueous solution was carried out when the absence of dissolved oxygen was needed. Mesoporous SiO_2 (SBA-15, Sigma-Aldrich) with average particle size of 150 μm and average pore size of 8 nm was used for the immobilization of fullerol. The SBA-15 was dispersed in an aqueous fullerol solution (50 μM), and pH was subsequently adjusted to 3 with $HClO_4$. After stirring for 5 h, the fullerol/SBA-15 was collected by filtering and was dried in an open-air oven (80 °C).

Photochemical Experiments. Photochemical experiments employed a 300 W Xe arc lamp (Oriel) as a light source and were performed in a 30 mL Pyrex reactor with a quartz window under air-equilibrated condition. Irradiation of visible light at an ambient temperature was achieved by passing light through a 10 cm IR water filter and a cutoff filter ($\lambda > 420$ nm). For measuring the wavelength-dependent photoactivities, a monochromator (Oriel) was used to vary the wavelength in the range of 400−640 nm. All monochromatic light intensities were measured to be 1.17 ± 0.15 mW cm^{-2} using a Power meter (Newport 1918-R). A typical solution of the photosensitizing system was prepared at a concentration of 100 μM RhB, 50 μM fullerol, and 50 μM substrate (4-CP, DCA, or TMA). The experimental solution was unbuffered in most cases, and the initial pH was adjusted to a desired value with 1 M $HClO_4$ or NaOH solution. On the other hand, the experiments to monitor FFA (100 μM) degradation at pH 7 were conducted in aqueous solutions of RhB and fullerol, buffered with 10 mM phosphate. Aliquots of 1 mL were intermittently withdrawn from the photoirradiated reactor using a 1 mL syringe and were transferred into a 2 mL amber glass vial (without filtration). Chemical reagents to quench any oxidants that might be produced during the reaction were not used. To confirm the reproducibility, the experiments were performed at least five times for any given condition.

Analysis. The concentrations of 4-CP and FFA were quantitatively analyzed using a high-performance liquid chromatograph (HPLC, Agilent 1260 Infinity) equipped with a diode array detector and a ZORBAX 300SB-C18 column (4.6 mm × 150 mm). The HPLC measurement of 4-CP was carried out using a binary mobile phase of 85% (v/v) aqueous phosphoric acid solution and acetonitrile (70:30 by volume), while FFA quantification was done using 40% aqueous methanol eluent. The ionic substrates and products were analyzed using a Dionex ion chromatograph (IC, Dionex DX-120) that was equipped with a conductivity detector and Dionex Ionpac CS-14 (4 mm × 250 mm) column for cation (TMA) analysis or AS-14 (4 mm × 250 mm) column for anion (DCA and Cl^-) analysis. For the cation analysis, 10 mM methanesulfonic acid was used, and for the anion analysis, 3.5 mM Na_2CO_3/1 mM $NaHCO_3$ was used. The removal of total organic carbon (TOC) in the visible light irradiated RhB/fullerol solution was monitored using a TOC analyzer (Shimadzu TOC-V_{SH}).

The production of $^{\bullet}OH$ was indirectly monitored using coumarin as a chemical trap of $^{\bullet}OH$, which is oxidatively converted into 7-hydroxycoumarin through the reaction with $^{\bullet}OH$. The hydroxylated product was quantified by measuring fluorescence emission intensity at 460 nm under the excitation at 332 nm.[18] RhB concentrations were spectrophotometrically determined by monitoring the absorbance at 554 nm (ε =

DOI: 10.1021/acs.est.6b03250
Environ. Sci. Technol. 2016, 50, 10545−10553

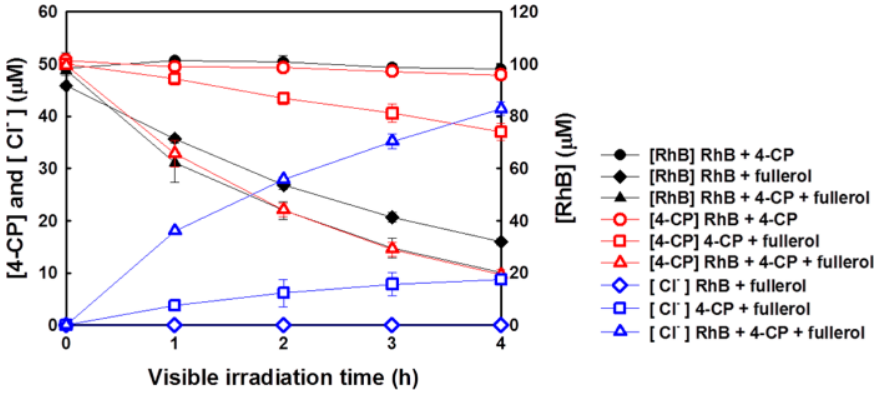

Figure 1. Fullerol-mediated RhB decolorization, 4-CP degradation, and Cl^- generation under visible light irradiation ($\lambda > 420$ nm) ($[fullerol]_0$ = 50 μM; $[RhB]_0$ = 100 μM; $[4\text{-CP}]_0$ = 50 μM; pH_i = 3.0; air-equilibrated).

13 500 M^{-1} cm^{-1}).[19] Photoluminescence emission spectra of RhB solution were measured using a spectrofluorometer (HORIBA, Fluoromax 4C-TCSPC). For electron paramagnetic resonance (EPR) analysis, 5,5-dimethyl-1-pyrroline-N-oxide (DMPO) and 2,2,6,6-tetramethyl-4-piperidone (TEMP) were used as a spin-trapping agent for radical species ($^{\bullet}OH$ and $^{\bullet}HO_2$) and $^1O_2$, respectively. The EPR spectra of ROS adducts were monitored using a JES-TE 300 spectrometer (JEOL, Japan). The EPR measurement conditions were as follows: microwave power, 3 mW; microwave frequency, 9.42 GHz; center field, 338.25 mT; modulation width, 0.2 mT; and modulation frequency, 100 kHz. UV/visible absorption spectra of fullerol solution and fullerol/SBA-15 (powder sample) were recorded using a spectrophotometer; Agilent 8453 and Shimadzu UV-2600 with an integrating sphere attachment were used. The diffuse reflectance spectra were obtained using $BaSO_4$ as a reference.

RESULTS AND DISCUSSION

Simultaneous RhB Decolorization and 4-CP Degradation by Fullerol. Figure 1 demonstrates that RhB decolorization proceeds concurrently with 4-CP degradation and the stoichiometric production of chloride ions under visible light irradiation ($\lambda > 420$ nm) when fullerol is present. The sensitized degradation of 4-CP was maximal at the concentration of [RhB] = 100 μM, which was employed in this study (see Figure S1). The solution pH was initially adjusted to 3 and was marginally changed in the course of photosensitized reaction. Neither direct photolysis nor dark adsorption on fullerol removed RhB and 4-CP at all (see Figure S2). Regardless of the presence of 4-CP, fullerol degraded RhB under visible light (Figure 1), which indicates that fullerol oxidizes RhB molecules as suggested in Scheme 1. Whereas the use of fullerol alone slightly degraded 4-CP through a direct electron transfer from 4-CP to $^3C_{60}(OH)_x^*$ (i.e., 4-CP + $^3C_{60}(OH)_x^* \rightarrow$ 4-$CP^{\bullet+}$ + $C_{60}(OH)_x^{\bullet-}$) under visible light irradiation, the degradation of 4-CP was significantly enhanced in the binary RhB/fullerol system. Some quinone compounds (e.g., benzoquinone (BQ), catechol (CC), hydroquinone (HQ), hydroxyhydroquinone (HHQ)) were detected as hydroxylated intermediates during the photosensitized degradation of 4-CP in the RhB/fullerol system (Figure S3a). However, such hydroxylated products of 4-CP degradation were not observed when fullerol alone was used as the sensitizer (Figure S3b). This implies that the interaction between excited fullerol and RhB molecules induces the production of $^{\bullet}OH$ (Scheme 1). $^{\bullet}OH$-induced oxidation of chlorophenols leads to the generation of chloride and other intermediates via multiple reaction pathways: (1) $^{\bullet}OH$ addition to the aromatic ring of chlorophenol to yield chlorodihydroxycyclohexadienyl (CDHCHD) radical, (2) the addition of O_2 to CDHCHD radical or the coupling and disproportional of two CDHCHD radicals, and (3) the subsequent rearrangement to release a chloride ion with the formation of various intermediates (e.g., hydroquinone and catechol).[20,21]

Figure 2 compares the efficiencies of the RhB/fullerol system for RhB decolorization and 4-CP degradation as a function of

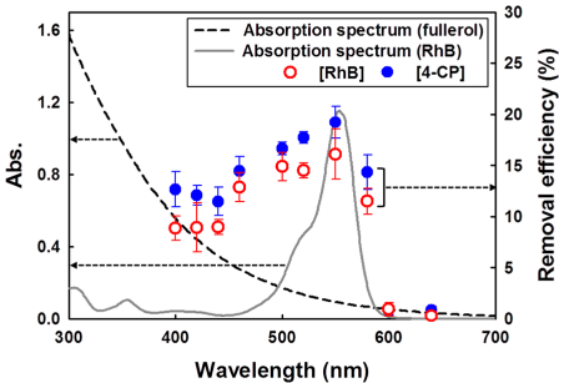

Figure 2. Simultaneous degradation of RhB and 4-CP in aqueous fullerol solution under different illumination wavelengths (controlled by a monochromator) for 4 h and the UV−vis absorption spectra of fullerol (dashed line) and RhB (solid line) ($[fullerol]_0$ = 50 μM; $[RhB]_0$ = 100 μM; $[4\text{-CP}]_0$ = 50 μM; pH_i = 3.0; air-equilibrated).

the irradiation wavelength that was controlled by a monochromator. The removal efficiencies of both RhB and 4-CP were the highest at 550 nm, which is in agreement with the absorption maximum of RhB spectrum. This indicates that the sensitization by RhB is important in the overall photochemical process. The photoexcited RhB can donate electrons to excited and ground states of $C_{60}(OH)_x$ under visible light. However, the photodegradation activities of RhB and 4-CP are also significant even at the wavelengths where RhB hardly absorbs (i.e., 400−460 nm region). This implies that not only the excited RhB but also the excited fullerol contributes to the overall photodegradation process as Scheme 1 shows. The comparison of reduction potentials ($E^0(^3C_{60}(OH)_x^*)$ = +1.10

DOI: 10.1021/acs.est.6b03250
Environ. Sci. Technol. 2016, 50, 10545−10553

V_{NHE} vs $E^0(C_{60}(OH)_x) = -0.20\ V_{NHE}$)[16] implies that $^3C_{60}(OH)_x^*$ is a stronger oxidant than its ground state.

Reaction Mechanisms. Photochemical degradation of 4-CP in the RhB/fullerol solution was tested under argon-saturated condition where the oxidant generation via O_2 reduction should not be possible. Very slow 4-CP decomposition occurred in the absence of O_2 (Figure 3a). The addition of chromate (i.e., Cr(VI)) as an alternative electron acceptor in the presence of dissolved O_2 also induced a marked retardation in the rate of 4-CP degradation (Figure 3a), which is attributable to the competition between chromate and dioxygen for electrons from $C_{60}(OH)_x^{\bullet-}$. This supports that the role of dioxygen as a precursor of oxidizing radicals (i.e., $O_2^{\bullet-}$, $^{\bullet}OH$) is critical for the oxidative degradation of 4-CP in the photosensitizing system. Despite the inhibition of ROS production, 4-CP was still degraded to a slight extent under anoxic condition or in the presence of chromate, which likely resulted from the one-electron oxidation of 4-CP by $^3C_{60}(OH)_x^*$. The oxidative transformation of phenolic compounds by the excited triplet states of sensitizers such as porphyrin[22] and humic[23] substances supports the nonradical mechanism involving $^3C_{60}(OH)_x^*$.

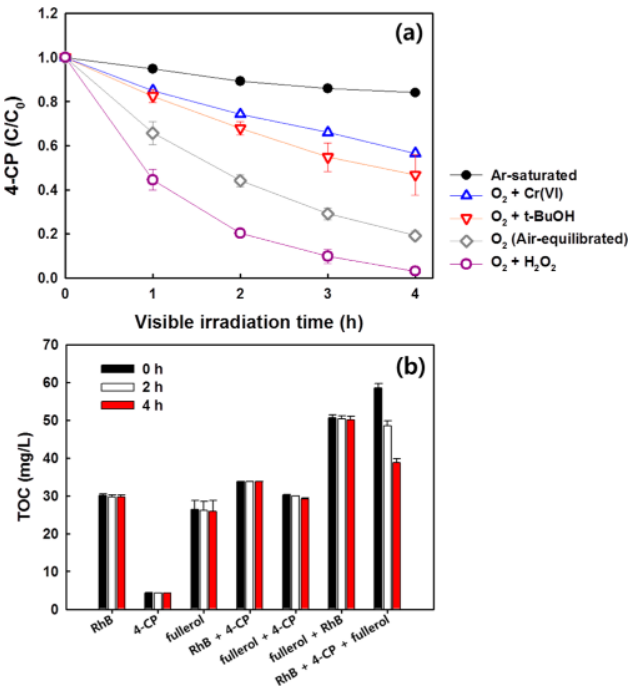

Figure 3. (a) Photosensitized degradation of 4-CP in RhB/fullerol solution: Effects of dissolved O_2 and added probe chemicals. (b) Change of TOC during 4 h visible light irradiation ($[fullerol]_0$ = 50 μM; $[RhB]_0$ = 100 μM; $[4\text{-CP}]_0$ = 50 μM; $[Cr(VI)]_0$ = 100 μM; $[t\text{-BuOH}]_0$ = 0.1 M; $[H_2O_2]$ = 1 mM; pH_i = 3.0; λ > 420 nm).

The transformation of dioxygen into hydroxyl radical may involve the production of H_2O_2 as an intermediate. Since the analysis of H_2O_2 by a common colorimetric method is not possible in the presence of RhB dye, we investigated the effect of H_2O_2 addition, which accelerated 4-CP degradation in the RhB/fullerol system, with $k = 0.86\ h^{-1}$ (with H_2O_2) vs $k = 0.41\ h^{-1}$ (without H_2O_2) (Figure 3a). This supports the possibility of H_2O_2 involvement as a nonradical intermediate during the successive O_2 reduction into $^{\bullet}OH$. On the other hand, the presence of excess t-BuOH as a hydroxyl radical scavenger decelerated the photosensitized degradation of 4-CP [$k = 0.20\ (\pm 0.03)\ h^{-1}$ (with t-BuOH)] (Figure 3a), which supports the visible light induced production of $^{\bullet}OH$ in the RhB/fullerol solution. However, the fact that the addition of 0.1 M t-BuOH did not completely inhibit the 4-CP degradation implies that the direct electron transfer from 4-CP to $^3C_{60}(OH)_x^*$ may contribute as an alternative oxidative degradation pathway (see the slight removal of 4-CP by fullerol alone (Figure 1)).[24,25] RhB decolorization was not retarded at all when t-BuOH was added (Figure S4), which suggests that RhB is oxidized predominantly via a direct electron transfer to $^3C_{60}(OH)_x^*$. The RhB/fullerol system was also examined for the degradation of DCA and TMA that are not reactive with $^1O_2$. In particular, TMA that is very recalcitrant against oxidative degradation can be degraded only by a strong oxidant like $^{\bullet}OH$.[26] Significant decomposition of DCA and TMA proceeded only in the mixture of RhB and fullerol (Figure S5) and was markedly decelerated in the presence of t-BuOH. Significant TOC reduction was not observed in any binary mixture (e.g., RhB/fullerol, 4-CP/fullerol, or RhB/4-CP) and only the ternary mixture, RhB/fullerol/4-CP, achieved the TOC removal of 19.7 mg/L after 4 h visible light irradiation (Figure 3b), which is likely attributed to $^{\bullet}OH$-induced mineralization of 4-CP.

To further corroborate the possible production of $^{\bullet}OH$ in the RhB/fullerol system, we monitored the formation of 7-hydroxycoumarin (eq 1) as a result of hydroxylation of coumarin (a probe of $^{\bullet}OH$) in the visible light irradiated solution containing RhB and fullerol.

$$^{\bullet}OH + \text{coumarin} \rightarrow \rightarrow \text{7-hydroxycoumarin} \quad (1)$$

Figure 4a shows that the production of 7-hydroxycoumarin proceeded 6-fold faster in the binary RhB/fullerol solution than in the presence of fullerol alone, which also indicates the involvement of $^{\bullet}OH$ as a major oxidant in 4-CP decomposition. The experimental conditions that inhibit the reductive conversion of O_2 (i.e., Ar-saturation, chromate (Cr(VI)) addition) significantly reduced the efficiency of 7-hydroxycoumarin generation (Figure 4a). The fact that the 7-hydroxycoumarin emission signal was not completely quenched in the Ar-saturated condition might be ascribed to a minor path of direct one-electron oxidation of coumarin by $^3C_{60}(OH)_x^*$ in which the resulting coumarin radical cation reacts with water molecule to generate the hydroxylated product. The addition of superoxide dismutase (SOD), which quenches superoxide (an intermediate to $^{\bullet}OH$), decreased the rate of 4-CP degradation, whereas it caused no retardation in RhB decoloration (Figure 4b).

Taken together, concomitant decolorization of RhB and oxidative degradation of organics (e.g., 4-CP, DCA, and TMA) proceed via multiple reaction pathways as follows. The electron exchange between excited and ground states of RhB and $C_{60}(OH)_x$ would result in the formation of a pair of radical cation and anion, $RhB^{\bullet+}$ and $C_{60}(OH)_x^{\bullet-}$ (eqs 2–4), which likely occurs in parallel with one-electron oxidation of 4-CP by $^3C_{60}(OH)_x^*$ (eq 5). The reaction route involving no ROS is based on the oxidizing power of $^3C_{60}(OH)_x^*$ ($E^0(^3C_{60}(OH)_x^*/C_{60}(OH)_x^{\bullet-}) = +1.10\ V_{NHE}$ vs $E^0(4\text{-}CP^{\bullet+}/4\text{-CP}) = +0.80\ V_{NHE}$). The dye radical cation undergoes further oxidation by O_2 (i.e., RhB decolorization).

$$RhB^* + C_{60}(OH)_x \rightarrow RhB^{\bullet+} + C_{60}(OH)_x^{\bullet-} \quad (2)$$

DOI: 10.1021/acs.est.6b03250
Environ. Sci. Technol. 2016, 50, 10545−10553

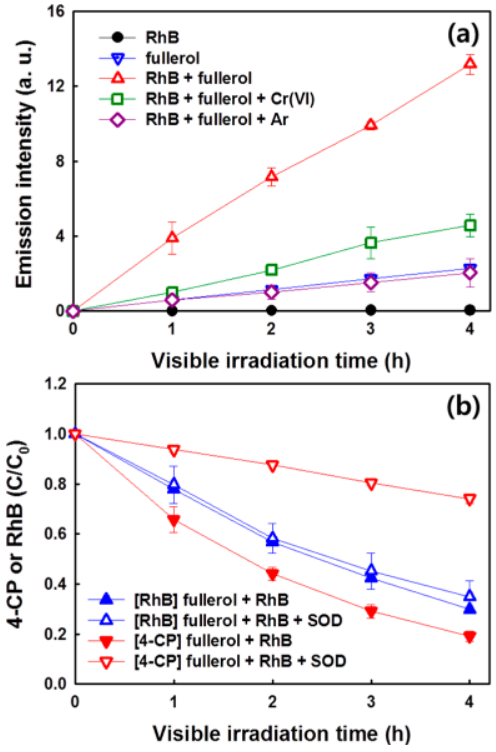

Figure 4. (a) Visible light induced production of 7-hydroxycoumarin as a coumarin−OH adduct (monitored by its photoluminescence) in the aqueous solutions of fullerol, RhB, and RhB/fullerol mixture in various conditions. (b) Simultaneous degradation of RhB and 4-CP in aqueous fullerol solutions in the absence and presence of SOD ($[fullerol]_0$ = 50 μM; $[RhB]_0$ = 100 μM; $[4\text{-CP}]_0$ = 50 μM; $[coumarin]_0$ = 1 mM; $[Cr(VI)]_0$ = 100 μM; $[SOD]_0$ = 66.7 mg/L; pH_i = 3.0; air-equilibrated except for the Ar-saturated case).

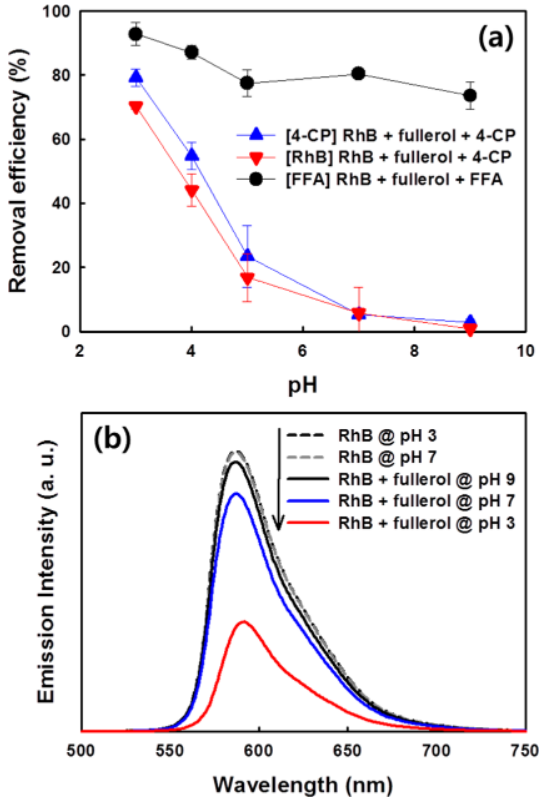

Figure 5. (a) Photosensitized degradation of RhB, 4-CP, and FFA in the RhB/fullerol solution as a function of initial pH ($[fullerol]_0$ = 50 μM; $[RhB]_0$ = 100 μM; $[4\text{-CP}]_0$ = 50 μM; $[FFA]_0$ = 100 μM). (b) The photoluminescence emission spectra of RhB in the absence and presence of fullerol at pH 3, 7, and 9 (λ_{ex} = 550 nm).

$$RhB^* + {}^3C_{60}(OH)_x^* \rightarrow RhB^{\bullet+} + C_{60}(OH)_x^{\bullet-} \quad (3)$$

$$RhB + {}^3C_{60}(OH)_x^* \rightarrow RhB^{\bullet+} + C_{60}(OH)_x^{\bullet-} \quad (4)$$

$$4\text{-CP} + {}^3C_{60}(OH)_x^* \rightarrow C_{60}(OH)_x^{\bullet-} + 4\text{-CP}^{\bullet+} \quad (5)$$

${}^3C_{60}(OH)_x^*$ contributes to the production of ROS in two ways: energy transfer versus electron transfer. The energy transfer from ${}^3C_{60}(OH)_x^*$ to dissolved oxygen leads to the formation of ${}^1O_2$ (eq 6). Alternatively, the oxidative power of ${}^3C_{60}(OH)_x^*$ to abstract electrons from either RhB or 4-CP enables the generation of $C_{60}(OH)_x^{\bullet-}$, which initiates the consecutive reduction of O_2 for the production of $^{\bullet}OH$ via $O_2^{\bullet-}$ (eq 7).

$${}^3C_{60}(OH)_x^* + {}^3O_2 \rightarrow C_{60}(OH)_x + {}^1O_2 \quad ({}^1O_2 \text{ formation}) \quad (6)$$

$$C_{60}(OH)_x^{\bullet-} + O_2 \rightarrow \rightarrow O_2^{\bullet-} \text{ and } {}^{\bullet}OH \quad (\text{oxidizing radical formation}) \quad (7)$$

pH-Dependent Reaction Mechanism. Figure 5a shows the rates of degradation of 4-CP and furfuryl alcohol (FFA) (as ${}^1O_2$ indicator[27]) in the RhB/fullerol solution as a function of initial pH. Whereas the photosensitizing activity for FFA decomposition remained relatively constant irrespective of pH, the efficiencies for RhB decolorization and 4-CP degradation drastically decreased with increasing pH. The different pH dependence of the photochemical degradation kinetics may be attributable to switching of the reaction pathway in response to pH change: singlet oxygenation versus $^{\bullet}OH$-induced oxidation. A significant reduction in the RhB and 4-CP decomposition occurred as the pH increased from 3 to 5, and further increase to pH 7 and pH 9 caused the negligible removal of RhB and 4-CP (Figure 5a). This pH-dependent behavior indicates that the production of $^{\bullet}OH$ is highly favored at acidic condition. Fullerol (pK_a = 4.0)[28] carries negative charges at neutral and alkaline condition, which makes the photoinduced electron transfer from the excited dye to negatively charged fullerol (eq 1) less favored at higher pH because of the electrostatic repulsion. In addition, the production of $^{\bullet}OH$ through the consecutive reduction of O_2 should be favored under proton-rich condition (acidic pH) (see eq 8). As a result, the hydroxyl radical-mediated mechanism should be dominant at acidic pH and less favored at alkaline condition.

$$O_2 + 3e^- + 3H^+ \rightarrow {}^{\bullet}OH + H_2O \quad (8)$$

On the other hand, ${}^1O_2$ production via energy transfer from ${}^3C_{60}(OH)_x^*$ to O_2 (eq 6) should be little affected by pH change, which caused FFA oxidation efficiency to be relatively independent of pH.

We monitored the photoluminescence (PL) intensity of the RhB/fullerol mixture as a function of initial pH (Figure 5b). Whereas the PL intensity of RhB (in the absence of fullerol) remained invariant irrespective of initial pH (pH 3 vs 7), the PL intensity of the RhB/fullerol mixture was markedly reduced when pH decreased from 7 to 3. Considering that the electron

DOI: 10.1021/acs.est.6b03250
Environ. Sci. Technol. 2016, 50, 10545−10553

transfer from RhB* should lower the PL intensity, the lower PL intensity at acidic pH in the RhB/fullerol solution implies that the electron transfer from RhB* to fullerol is favored at acidic pH. This is also consistent with the higher photodegradation activity at acidic pH (Figure 5a). Acidic condition favors the direct electron transfer from RhB* to fullerol (leading to $^{\bullet}OH$ production), whereas it is not favored in the basic pH region.

To further characterize the production of $^1O_2$ under varying pH condition, we performed the photochemical degradation of FFA in the solution of fullerol alone (Figure 6a) and RhB/fullerol (Figure 6b) in the presence of t-BuOH or L-histidine (as $^1O_2$ scavenger[26,29]) at acidic and neutral pH region. Regardless of the initial pH, the addition of L-histidine caused a drastic decrease in FFA degradation efficiency in fullerol alone solution, while no such marked retardation was observed with the addition of t-BuOH (Figure 6a). This confirms that $^1O_2$ (generated via eq 6) works as a main oxidant in the fullerol-sensitized system. When a binary mixture of RhB and fullerol was used as the photosensitizing system, the effects of L-histidine and t-BuOH were similar to Figure 6a at pH 7 but were reversed at pH 3 (Figure 6b). t-BuOH showed a much more pronounced quenching effect at pH 3 than L-histidine, which suggests that FFA was oxidized mainly by nonselective $^{\bullet}OH$ in the binary RhB/fullerol system at pH 3. On the other hand, the presence of L-histidine almost completely inhibited FFA decomposition at pH 7, whereas FFA was still significantly degraded when t-BuOH was added instead. This implies a role of $^1O_2$ as a dominant oxidant in the RhB/FFA system at neutral pH. This could be further verified by comparing FFA degradation rates in deuterated water (Figure S6). At neutral pH condition where $^1O_2$ acts as a major oxidant in the RhB/fullerol solution, the alternative use of D_2O solvent that is less efficient in $^1O_2$ deactivation (i.e., $k_d(D_2O) = 1.6 \times 10^4\ s^{-1}$; $k_d(H_2O) = 2.4 \times 10^5\ s^{-1}$)[30] accelerated the rate of FFA decomposition, with $k = 1.87\ h^{-1}$ in D_2O versus $k = 0.42\ h^{-1}$ in H_2O.

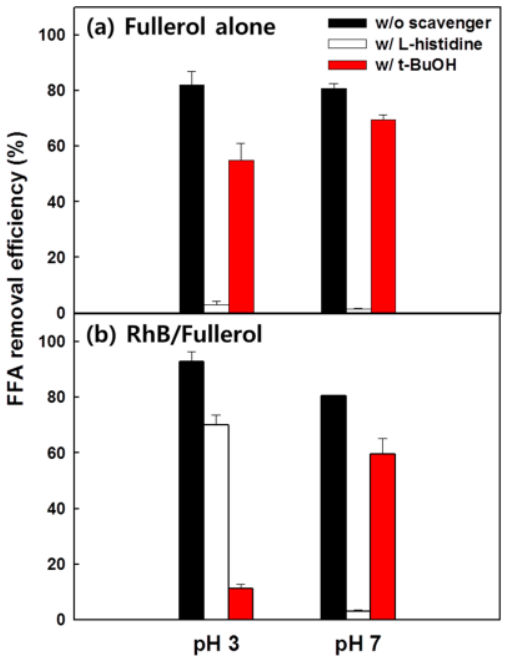

Figure 6. Photochemical degradation of FFA in the solution of (a) fullerol alone and (b) RhB/fullerol solution in the absence and presence of L-histidine ($^1O_2$ scavenger) or t-BuOH ($^{\bullet}OH$ scavenger) ([fullerol]$_0$ = 50 μM; [RhB]$_0$ = 100 μM; [FFA]$_0$ = 100 μM; [L-histidine]$_0$ = 10 mM; [t-BuOH]$_0$ = 0.1 M; [phosphate]$_0$ = 10 mM).

Using EPR spin-trapping technique, we detected oxidizing radicals such as $^{\bullet}OH$ and $HO_2^{\bullet}$ (hydroperoxyl radical) and $^1O_2$ in the RhB/fullerol solution, which is shown in Figure 7. The

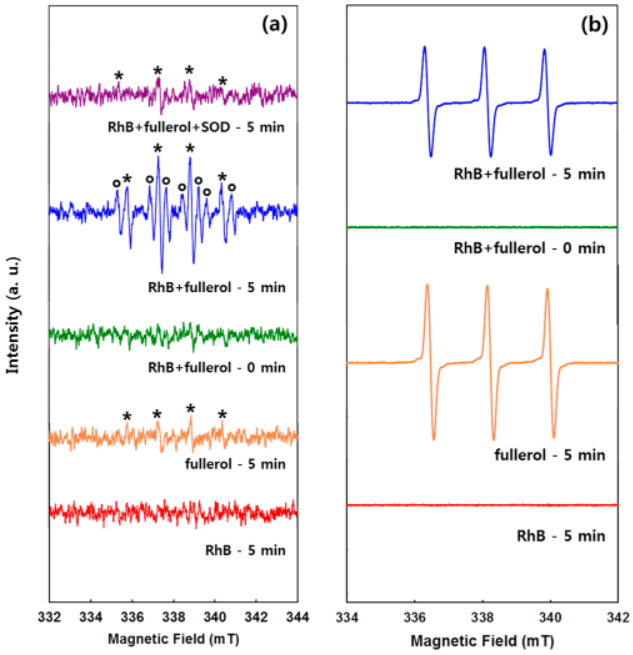

Figure 7. EPR spectra of (a) OH−DMPO (*) and OOH−DMPO (deg) adducts (at pH 3) and (b) $^1O_2$-TEMP adduct (at pH 7) obtained under visible light irradiation of RhB, fullerol, and the binary mixture ([fullerol]$_0$ = 0.33 mM; [RhB]$_0$ = 0.33 mM; [DMPO]$_0$ = [TEMP]$_0$ = 0.17 M; [SOD]$_0$ = 66.7 mg/L; [phosphate]$_0$ = 10 mM; air-equilibrated).

peaks characteristic of DMPO−OH and DMPO−OOH in the EPR spectra ensure that successive electron transfers from $C_{60}(OH)_x^{\bullet-}$ to dioxygen result in the formation of $^{\bullet}OH$ via $O_2^{\bullet-}$ (eq 7) at acidic condition (pH 3). In particular, when SOD as a superoxide quencher was added to the RhB/fullerol solution, the peak intensities corresponding to $HO_2^{\bullet}$ and $^{\bullet}OH$ were significantly reduced. This confirms that $HO_2^{\bullet}$ (or $O_2^{\bullet-}$) is a critical intermediate to $^{\bullet}OH$ formation and is consistent with the finding that 4-CP degradation was inhibited in the presence of SOD (Figure 4b). The signals for TEMP−$^1O_2$ adducts shown in Figure 7b also confirm the sensitized production of $^1O_2$ at pH 7. They were observed even in the absence of RhB, which assures that the singlet oxygen is generated by the sensitization of fullerol alone as illustrated in Scheme 1.

Overall, all the earlier pH-dependent results corroborate that fullerol mediates the electron transfer to accelerate the photosensitized production of $^{\bullet}OH$ in the presence of RhB preferably at acidic condition and enhances the energy transfer to generate $^1O_2$ in the absence of RhB dominantly at neutral condition.

Immobilized Fullerol and System Stability. C_{60} derivatives were immobilized on the surface of functionalized and mesoporous silica supports to prevent their aggregation and to recycle them after photochemical reaction.[31] The surface

DOI: 10.1021/acs.est.6b03250
Environ. Sci. Technol. 2016, 50, 10545−10553

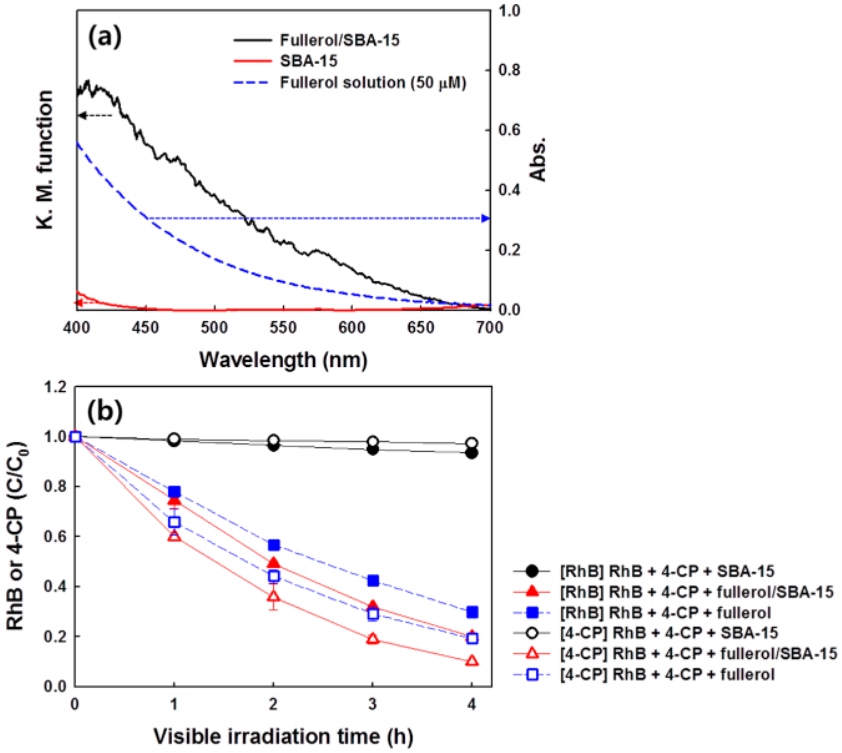

Figure 8. (a) The diffuse reflectance UV/vis spectrum of fullerol-immobilized SBA-15. The absorption spectrum of fullerol was obtained from the aqueous solution while those of fullerol/SBA-15 and SBA-15 were the diffuse reflectance spectrum of powder samples. Therefore, two spectra cannot be directly compared. (b) Simultaneous decolorization of RhB and degradation of 4-CP on fullerol-immobilized SBA-15 under visible light ($\lambda > 420$ nm) ($[SBA\text{-}15]_0 = [fullerol/SBA\text{-}15]_0 = 0.5$ g/L; $[fullerol]_0 = 50$ μM; $[RhB]_0 = 100$ μM; $[4\text{-}CP]_0 = 50$ μM; $pH_i = 3.0$). The fullerol loading on SBA-15 was estimated to be 70 mg/g·SBA-15).

of C_{60} derivatives and solid supports should be modified by various chemical functional groups such as amine[32] and carboxylic acid[33] for stable immobilization. However, fullerol can be easily immobilized on the surface of mesoporous silica through a hydroxyl group without further chemical treatments (Figure 8a). Figure 8b shows that concomitant degradation of RhB and 4-CP was pronounced using fullerol-loaded SBA-15 (fullerol/SBA-15) under visible light irradiation, while the use of bare SBA-15 did not cause any removal of RhB or 4-CP. Neither RhB nor 4-CP was adsorbed on fullerol/SBA-15 in the dark condition, and the addition of 4-CP did not change the absorption spectrum of fullerol/SBA-15 at all, which confirms little interaction between 4-CP and fullerol/SBA-15 (Figure S7). The heterogeneous photocatalytic activity of fullerol/SBA-15 was comparable to that of the homogeneous counterpart.

The photostability of aqueous fullerol and fullerol/SBA-15 was evaluated by carrying out repeated cycles of 4-CP degradation and RhB decolorization in the same batch of the reactor (Figure S8). Fullerol immobilized on SBA-15 showed stronger stability and better performance than water-soluble fullerol during the repeated uses. Although both heterogeneous and homogeneous systems underwent gradual loss of photosensitizing activity during the multiple uses, the fullerol/SBA-15 showed 25% activity reduction whereas water-soluble fullerol exhibited 45% reduction after five cycles under the same reaction conditions. This deactivation seems to be largely caused by the gradual loss of fullerol by samplings and the gradual accumulation of substrates (4-CP and RhB) and their degradation intermediates. Although a partial deactivation of fullerol cannot be ruled out, the activity of fullerol is largely maintained throughout multiple cycles.

Environmental Applications. This study demonstrates the first instance of visible light sensitized production of $^{\bullet}OH$ as a result of fullerol-mediated electron transfer from the photoexcited dye to dissolved oxygen. Such $^{\bullet}OH$-producing mechanism enables the degradation and mineralization of recalcitrant compounds such as 4-CP, DCA, and TMA under visible light irradiation, which is not possible with the $^1O_2$-based mechanism that most fullerene-based photochemical oxidation systems follow. The proposed photosensitizing process achieves dye decoloration and pollutant mineralization simultaneously. The results imply that fullerol (or fullerene derivatives) may work similarly to produce $^{\bullet}OH$ through mediating electron transfer in the presence of natural organic matters as a photosensitizer. Such a possibility needs to be tested in further studies. Other combinations of dyes and sensitizers with fullerene derivatives also need to be investigated to test the general applicability of the proposed concept. The photooxidation mechanism depending on pH is an advantage since the main working oxidant can be switchable between $^1O_2$ and $^{\bullet}OH$. The selective $^1O_2$ undergoes limited quenching by background organic matters,[34] while $^{\bullet}OH$ with strong oxidizing power enables the degradation of a broad range of organic compounds.[35]

ASSOCIATED CONTENT

* Supporting Information

The Supporting Information is available free of charge on the ACS Publications website at DOI: 10.1021/acs.est.6b03250.

DOI: 10.1021/acs.est.6b03250
Environ. Sci. Technol. 2016, 50, 10545−10553

Optimization of RhB concentration for visible light activity (Figure S1), direct photolysis under visible light and dark control data (Figure S2), intermediates produced from 4-CP degradation (Figure S3), effect of t-BuOH addition on the photosensitized degradation of RhB (Figure S4), photodegradation of DCA and TMA in the RhB/fullerol solution (Figure S5), photosensitized oxidation of FFA in D_2O (Figure S6), dark reaction of fullerol/SBA-15 and absorption spectra of fullerol/SBA-15 before and after 4-CP adsorption (Figure S7), repeated cycles of 4-CP, and RhB photodegradation in the presence of aqueous fullerol and fullerol/SBA-15 (Figure S8)
(PDF)

AUTHOR INFORMATION

Corresponding Authors
* E-mail: wchoi@postech.edu; phone: +82-54-279-2283.
* E-mail: lee39@korea.ac.kr; phone: +82-2-3290-4864.

Notes
The authors declare no competing financial interest.

ACKNOWLEDGMENTS

This work was supported by the Global Research Laboratory (GRL) Program (No. NRF-2014K1A1A2041044), KCAP (Sogang Univ.) (No. 2009-0093880), and Basic Science Research Program (2014R1A1A2056935) which were funded by the Korea Government (MSIP) through the National Research Foundation (NRF). Partial funding was provided by the NSF ERC on Nanotechnology-Enabled Water Treatment (EEC-1449500) and Human Resources Program in Energy Technology of KETEP (No. 20144030200460).

REFERENCES

(1) Ballatore, M. B.; Durantini, J.; Gsponer, N. S.; Suarez, M. B.; Gervaldo, M.; Otero, L.; Spesia, M. B.; Milanesio, M. E.; Durantini, E. N. Photodynamic inactivation of bacteria using bovel electrogenerated porphyrin-fullerene C_{60} polymeric films. Environ. Sci. Technol. 2015, 49, 7456−7463.
(2) Vileno, B.; Marcoux, P. R.; Lekka, M.; Sienkiewicz, A.; Feher, T.; Forro, L. Spectroscopic and photophysical properties of a highly derivatized C_{60} fullerol. Adv. Funct. Mater. 2006, 16, 120−128.
(3) Yamakoshi, Y.; Sueyoshi, S.; Fukuhara, K.; Miyata, N. $^{\bullet}OH$ and $O_2^{\bullet-}$ generation in aqueous C_{60} and C_{70} solutions by photoirradiation: An EPR study. J. Am. Chem. Soc. 1998, 120, 12363−12364.
(4) Yamakoshi, Y.; Umezawa, N.; Ryu, A.; Arakane, K.; Miyata, N.; Goda, Y.; Masumizu, T.; Nagano, T. Active oxygen species generated from photoexcited fullerene (C_{60}) as potential medicines: $O_2^{\bullet-}$ versus $^1O_2$. J. Am. Chem. Soc. 2003, 125, 12803−12809.
(5) Lee, J.; Fortner, J. D.; Hughes, J. B.; Kim, J-H. Photochemical production of reactive oxygen species by C_{60} in the aqueous phase during UV irradiation. Environ. Sci. Technol. 2007, 41, 2529−2535.
(6) Hotze, E. M.; Badireddy, A. R.; Chellam, S.; Wiesner, M. R. Mechanisms of bacteriophage inactivation via singlet oxygen generation in UV illuminated fullerol suspensions. Environ. Sci. Technol. 2009, 43, 6639−6645.
(7) Lee, J.; Mackeyev, Y.; Cho, M.; Li, D.; Kim, J-H.; Wilson, L. J.; Alvarez, P. J. J. Photochemical and antimicrobial properties of novel C_{60} derivatives in aqueous systems. Environ. Sci. Technol. 2009, 43, 6604−6610.
(8) Pickering, K. D.; Wiesner, M. R. Fullerol-sensitized production of reactive oxygen species in aqueous solution. Environ. Sci. Technol. 2005, 39, 1359−1365.
(9) Hotze, E. M.; Labille, J.; Alvarez, P.; Wiesner, M. R. Mechanisms of photochemistry and reactive oxygen production by fullerene suspensions in water. Environ. Sci. Technol. 2008, 42, 4175−4180.
(10) Cho, M.; Fortner, J. D.; Hughes, J. B.; Kim, J-H. Escherichia coli inactivation by water-soluble, ozonated C_{60} derivative: Kinetics and mechanisms. Environ. Sci. Technol. 2009, 43, 7410−7415.
(11) Jafvert, C. T.; Kulkarni, P. P. Buckminsterfullerene's (C_{60}) octanol-water partition coefficient (K_{ow}) and aqueous solubility. Environ. Sci. Technol. 2008, 42, 5945−5950.
(12) Badireddy, A. R.; Hotze, E. M.; Chellam, S.; Alvarez, P.; Wiesner, M. R. Inactivation of Bacteriophages via photosensitization of fullerol nanoparticles. Environ. Sci. Technol. 2007, 41, 6627−6632.
(13) Choi, Y.; Ye, Y.; Mackeyev, Y.; Cho, M.; Lee, S.; Wilson, L. J.; Lee, J.; Alvarez, P. J. J.; Choi, W.; Lee, J. C_{60} aminofullerene-magnetite nanocomposite designed for efficient visible light photocatalysis and magnetic recovery. Carbon 2014, 69, 92−100.
(14) Lee, J.; Hong, S.; Mackeyev, Y.; Lee, C.; Chung, E.; Wilson, L. J.; Kim, J-H.; Alvarez, P. J. J. Photosensitized oxidation of emerging organic pollutants by tetrakis C_{60} aminofullerene-derivatized silica under visible light irradiation. Environ. Sci. Technol. 2011, 45, 10598−10604.
(15) Sawyer, D. T.; Valentine, J. S. How super Is superoxide? Acc. Chem. Res. 1981, 14, 393−400.
(16) Ge, L.; Moor, K.; Zhang, B.; He, Y. L.; Kim, J-H. Electron transfer mediation by aqueous C_{60} aggregates in H_2O_2/UV advanced oxidation of indigo carmine. Nanoscale 2014, 6, 13579−13585.
(17) Honda, S.; Ohkita, H.; Benten, H.; Ito, S. Multi-colored dye sensitization of polymer/fullerene bulk heterojunction solar cells. Chem. Commun. 2010, 46, 6596−6598.
(18) Kim, J.; Lee, C. W.; Choi, W. Platinized WO_3 as an environmental photocatalyst that generates OH radicals under visible light. Environ. Sci. Technol. 2010, 44, 6849−6854.
(19) Bae, S.; Kim, S.; Lee, S.; Choi, W. Dye decolorization test for the activity assessment of visible light photocatalysts: Realities and limitations. Catal. Today 2014, 224, 21−28.
(20) Dec, J.; Bollag, J. M. Dehalogenation of chlorinated phenols during oxidative coupling. Environ. Sci. Technol. 1994, 28 (3), 484−490.
(21) Stafford, U.; Gray, K.; Kamat, P. Radiolytic and TiO_2-assisted photocatalytic degradation of 4-chlorophenol. A comparative study. Dendrimer-fullerenol soft-condensed nanoassembly. J. Phys. Chem. 1994, 98, 6343−6351.
(22) Kim, W.; Park, J.; Jo, H. J.; Kim, H.-J.; Choi, W. Visible light photocatalysis based on homogeneous and heterogenized tin porphyrins. J. Phys. Chem. C 2008, 112 (2), 491−499.
(23) Wenk, J.; Aeschbacher, M.; Sander, M.; Gunten, U. V.; Canoica, S. Photosensitizing and inhibitory effects of ozonated dissolved organic matter on triplet-induced contaminant transformation. Environ. Sci. Technol. 2015, 49 (14), 8541−8549.
(24) Park, Y.; Singh, N. J.; Kim, K. S.; Tachikawa, T.; Majima, T.; Choi, W. Fullerol-titania charge-transfer-mediated photocatalysis working under visible light. Chem. - Eur. J. 2009, 15, 10843−10850.
(25) Lim, J.; Monllor-Satoca, D.; Jang, J. S.; Lee, S.; Choi, W. Visible light photocatalysis of fullerol-complexed TiO_2 enhanced by Nb doping. Appl. Catal., B 2014, 152−153, 233−240.
(26) Kim, S.; Hwang, S.-J.; Choi, W. Visible Light Active Platinum-Ion-Doped TiO_2 Photocatalyst. J. Phys. Chem. B 2005, 109, 24260−24267.
(27) Haag, W. R.; Hoigne, J. Singlet oxygen in surface waters 0.3. Photochemical formation and steady state concentrations in various types of waters. Environ. Sci. Technol. 1986, 20, 341−348.
(28) Bhattacharya, P.; Kim, S. H.; Chen, P. Y.; Chen, R.; Spuches, A. M.; Brown, J. M.; Lamm, M. H.; Ke, P. C. Dendrimer-fullerenol soft-condensed nanoassembly. J. Phys. Chem. C 2012, 116, 15775−15781.
(29) Cho, M.; Snow, S. D.; Hughes, J. B.; Kim, J-H. Escherichia coli inactivation by UVC-irradiated C_{60}: Kinetics and mechanisms. Environ. Sci. Technol. 2011, 45, 9627−9633.
(30) Wilkinson, F.; Helman, W. P.; Ross, A. B. Rate constants for the decay and reactions of the lowest electronically excited singlet-state of

DOI: 10.1021/acs.est.6b03250
Environ. Sci. Technol. 2016, 50, 10545−10553

molecular-oxygen in solution-An Expanded and revised compilation. J. Phys. Chem. Ref. Data 1995, 24, 663−1021.
(31) Moor, K. J.; Valle, D. C.; Li, C.; Kim, J.-H. Improving the Visible Light Photoactivity of Supported Fullerene Photocatalysts through the Use of [C_{70}] Fullerene. Environ. Sci. Technol. 2015, 49, 6190−6197.
(32) Moor, K. J.; Kim, J.-H. Simple Synthetic Method Toward Solid Supported C_{60} Visible Light-Activated Photocatalysts. Environ. Sci. Technol. 2014, 48, 2785−2791.
(33) Latassa, D.; Enger, O.; Thilgen, C.; Habicher, T.; Offermanns, H.; Diederich, F. Polysiloxane-supported fullerene derivative as a new heterogeneous sensitiser for the selective photooxidation of sulfides to sulfoxides by $^1O_2$. J. Mater. Chem. 2002, 12, 1993−1995.
(34) Kim, H.; Kim, W.; Mackeyev, Y.; Lee, G. S.; Kim, H. J.; Tachikawa, T.; Hong, S.; Lee, S.; Kim, J.; Wilson, L. J.; Majima, T.; Alvarez, P. J. J.; Choi, W.; Lee, J. Selective oxidative degradation of organic pollutants by singlet oxygen-mediated photosensitization: Tin porphyrin versus C_{60} aminofullerene systems. Environ. Sci. Technol. 2012, 46, 9606−9613.
(35) Buxton, G. V.; Greenstock, C. L.; Helman, W. P.; Ross, A. B. Critical review of rate constants for reactions of hydrated electrons, hydrogen atoms and hydroxyl radicals ($OH^{\bullet}/O^{\bullet-}$) in aqueous solution. J. Phys. Chem. Ref. Data 1988, 17, 513−886.

DOI: 10.1021/acs.est.6b03250
Environ. Sci. Technol. 2016, 50, 10545−10553